Magnetic Nanoparticles Synthesised by Ion-Implantation

A.E. Malik[a], K. Belay[b], D. Llewellyn[b], W.D. Hutchison[a], K. Nishmura[c] and R. Elliman[b]

[a] *School of Physical, Environmental and Mathematical Sciences, The University of New South Wales at ADFA, Canberra ACT 2600.*
[b] *Electronic Materials Engineering Department, Research School of Physics and Engineering, Australian National University, Canberra, ACT 0200, Australia .*
[c]*Graduate School of Science and Engineering, University of Toyama, Toyama, Japan*

Nanoparticles of metallic cobalt, platinum and a CoPt alloy have been synthesized, via ion implantation and thermal annealing, within 100 nm silica thin films thermally grown on silicon substrates. The size and spatial distributions of the nanoparticles are determined from transmission electron microscopy of sample cross-sections and the crystal structure form glancing angle X-ray diffraction analysis. These results are correlated with magnetisation measurements on the same samples.

1. Introduction

Ion implantation is a versatile technique for studying the synthesis and properties of nanosized metal particles in different host materials [1]. In particular, it is a non-equilibrium process that can be used to introduce metallic species into a host material at concentrations well above their equilibrium solubility limit. It also provides the flexibility to choose particular metallic species or combinations of species for investigation. The purpose of the present study is to investigate the synthesis and magnetic properties of Co, Pt and Co-Pt alloy nanoparticles in silica.

Cobalt, a well known magnetic material for data storage applications, has been paid special attention for the past few years, particularly with regard to the evolution of magnetic properties with the clusters sizes, and super-paramagnetic behaviour [2]. Co-Pt alloy films with a face-centred tetragonal structure have long been considered the bench mark for ultrahigh density magnetic recording media [3,4]. However, less attention has been paid to the production of Co-Pt alloy nanoparticles or their magnetic properties.

In this paper we report the formation of nanoparticles of Co, Pt and a 50% Co 50% Pt alloy in silica via implantation and subsequent thermal treatment. Magnetisation measurements and analysis of the structure and particle size distributions of these samples were undertaken and comparisons made between the three different kinds of nanoparticles.

2. Sample preparation

The starting substrate consisted of a 100 nm SiO_2 layer thermally grown on (100) oriented Si wafers. Separate regions of the silica layer were implanted with 50 keV Co ions or 100 keV Pt ions with fluences of 6×10^{16} ions/cm^2, or for the Co-Pt alloy, sequentially implanted with Co and then Pt ions each with a fluences of 3×10^{16} ions/cm^2. According to the Monte-Carlo ion-range simulation code SRIM 2007 [5], the average range of both Co and Pt ions in SiO_2 is ~43 nm for the above mentioned energies.

After implantation the samples were annealed at 900 ^{o}C in a nitrogen atmosphere for one hour. Implantation fluences and depths were confirmed with Rutherford backscattering spectrometry (RBS) using 2 MeV He^+ ions. The size and spatial distributions of the nanoparticles were measured by transmission electron microscopy (TEM) of sample cross-sections, and the crystal structure of the nanoparticles was determined from glancing angle x-

ray diffraction measurements. Magnetisation was measured using a SQUID magnetometer in hystersis mode. In the latter case, the substrates were thinned to ~ 100 μm to reduce the diamagnetic contribution from silicon.

3. Results and Discussion

A systematic structural and compositional investigation was carried out on the samples using TEM. Fig. 1 shows bright-field, cross-sectional images for sa mples implanted with Co, Pt and Co+Pt after one hour annealing in N_2 at 900ºC. In all the cases investigated, well defined spherical particles with dimensions in the sub-50nm range can be observed. It is evident from the images that size and size distributions are very different in the three cases, depending explicitly on the implanted species.

Supersaturated solid solutions, such as those produced by ion-implantation, are metastable and given sufficient atomic mobility (i.e. temperature and time) the excess solute atoms diffuse and cluster. The rate of cluster formation and the size-distribution of the resulting clusters are described by the classical theory of homogeneous nucleation [6, 7], at least for low levels of supersaturation. This theory is, however, based on many assumptions, including that the system is dilute, homogeneous and of infinite extent. In contrast, implanted samples typically have relatively high impurity concentrations (several at. %), spatial distributions that are finite and depth-dependent and matrices with finite dimensions. There is also the added possibility of impurity clustering, or pre-nucleation, during implantation, particularly around the peak of the implant distribution where the concentration is highest. As a consequence, nanocrystals produced in ion-implanted samples are usually found to have spatially-dependent size distributions, with larger precipitates forming around the peak of the implant distribution and smaller ones at the extremes of the distribution [8]. Effects due to finite extent of the materials are also observed, as is evident from the images in Fig. 1.

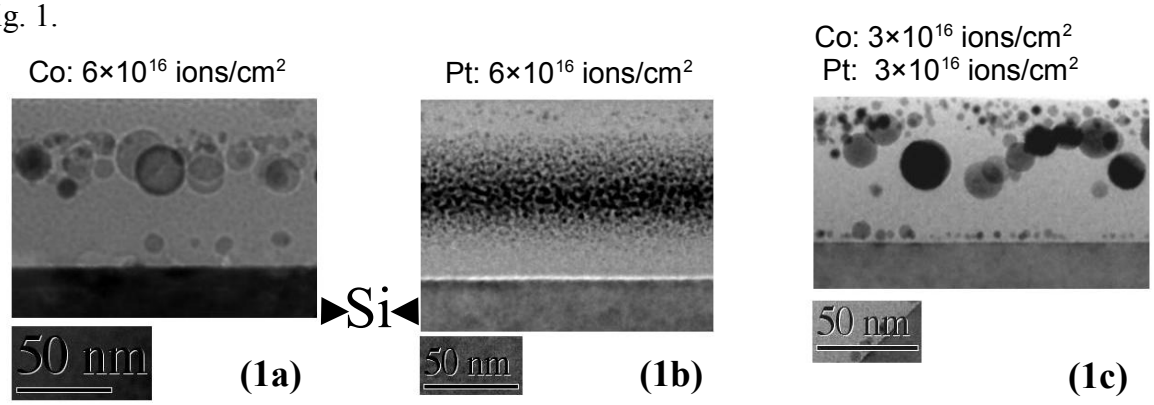

Fig. 1. TEM images for Co (1a), Pt (1b) and Co-Pt (1c) implanted samples annealed at 900 ºC for one hour.

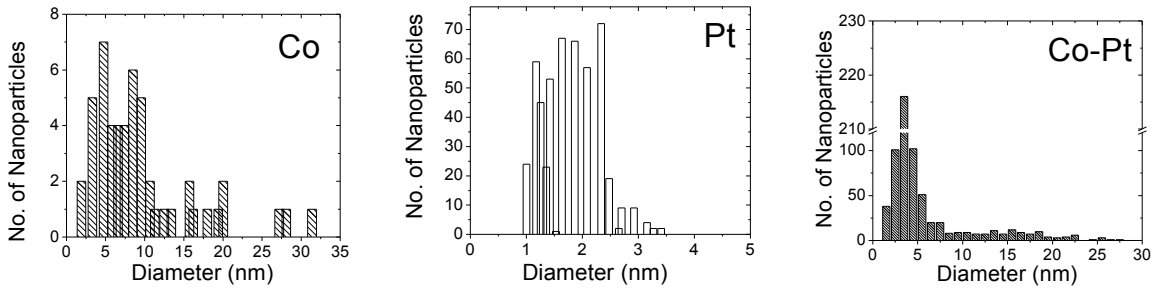

Fig. 2. Comparison between size distribution of Co, Pt and Co-Pt nanoparticles.

Fig. 2 shows the size distributions of nanoparticles in 100 nm silica after annealing, as determined from images such as those depicted in Fig. 1. Co formed the largest nanoparticles with average size of 6.4 nm. Interestingly, long range diffusion of the Co was also observed in these samples giving rise to nanocrystals in the vicinity of the SiO_2-Si interface. Pt formed very small nanoparticles (average diameter of 1.6 nm), which do not grow significantly during annealing. This suggests that Pt has a very low diffusivity at the annealing temperature employed for synthesis. The CoPt alloy sample shows the presence of nanoparticles both closer to the surface and at the SiO_2/Si interface. There farction of smaller nanoparticles is greater and more nanoparticles are present at the SiO_2/Si interface as compared to Co sample. The largest nanoparticles are of a similar size to the Co sample.

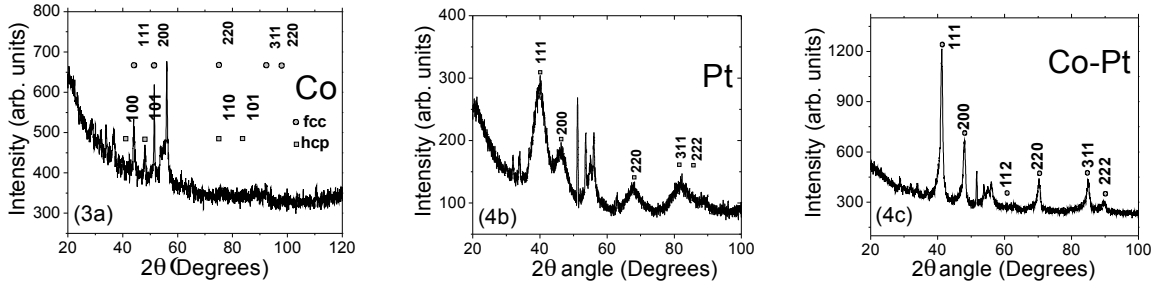

Fig. 3. XRD patterns of Co, Pt and Co-Pt nanoparticles fabricated by implantation and annealing at 900 °C.

All the samples were also examined by grazing incident x-ray diffraction. Fig. 3a shows that the Co is present in two different phases. A peak at 44.2° and a relatively smaller peak at 47.5° are signature peaks for fcc (111) and hcp (101) phases of Co. As-implanted samples exhibit very small Co nanocrystals with an hcp structure [9]. G. Mettei et al. [10] showed that more fcc Co spots appear in SAED pattern by "in situ" annealing of Co implanted sample in silica at 900° C. This implies that as the annealing temperature increases above 800°C, Co particles grow larger in size and their phase also changes from hcp to fcc. Additional peaks are also visible for 2Θ lower than 40°. These are likely due to the presence of crystalline cobalt silicate and possibly to some amount of cobalt oxide [11, 12]. The peaks between 50° and 57° degrees are due to the substrate and are present in all the patterns. The Pt XRD pattern has peaks consistent with the presence of a cubic phase with all prominent peaks at 39.8°, 46.3°, 67.5° and 81.3° being present. The CoPt alloy sample shows spectra consistent with a face centred tetragonal (fct) structure. The reflections at 2Θ values of 41.5 °, 47.6°, 60.8°, 71.03°, 84.7° and 90.14° arise from the (111), (200), (112), (202) (311) and (222) planes of the fct Co-Pt alloy phase.

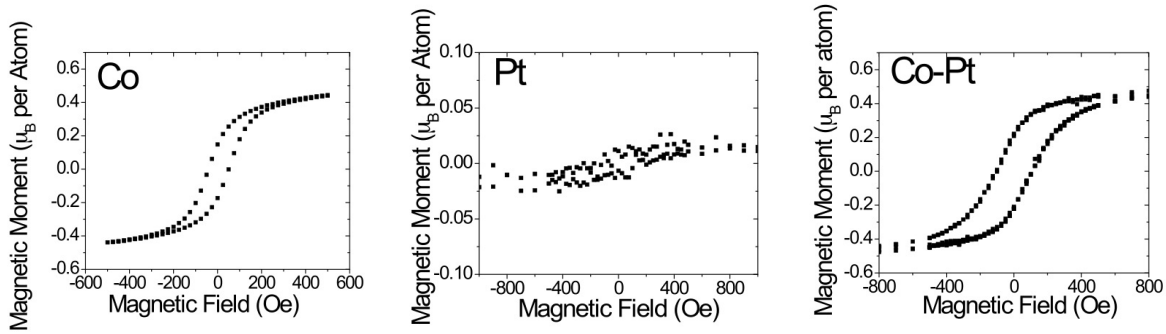

Fig. 4. Magnetisation measurements for the 3 samples at room temperature.

SQUID magnetometry was used to show and characterise the ferromagnetic behaviour of the nanoparticles. Hysteresis loops were collected at room temperature and up to ±3000 Oe. The resulting data for the Co, Pt and CoPt cases are shown in Fig.4. Here the magnetic moment per atom was calculated based on the nominal implanted fluence and the curves are truncated at ±900 Oe since saturation is essentially achieved at this modest applied field. The value of the saturated magnetic moment (~0.5 μ_B per atom) and the remanence is almost the same for the Co and CoPt alloy samples whereas it is nearly zero for the Pt sample. Interestingly however, the remanence M_R and the coercive field H_C are considerably larger for CoPt (M_R=0.215 μ_B/atom and H_C=107.15 Oe) compared with (M_R=0.16 μ_B/atom and H_C=46.4 Oe) for Co.

4. Conclusions:

Co, Pt and CoPt alloy nanoparticles were successfully produced using ion implantation and annealing. Due to the high diffusivity of Co and the relatively low diffusivity of Pt in silica, Co and CoPt-alloy nanoparticles were found to be larger than Pt-only nanoparticles. The high diffusivity of Co also led to the formation of Co-based nanoparticles at the SiO_2/interface in Co and CoPt implanted samples. Co nanoparticles were present as fcc and hcp phases while Pt and Co-Pt were fcc and fct phases, respectively. Both the Co and CoPt samples were observed to be ferromagnetic at room temperature with similar saturated moments and remanence. However the fct structured CoPt exhibited larger coercivity.

References

[1] Gilliot M, En Naciri A, Johann L, Stoquert J P, Grob J J and Muller D 2007 *J. Appl. Phys.* **101** 014319
[2] Orleans C D, Cerruti C, Estournes C, Grob C J J, Guille J L, Haas F, Muller D, Richard Plouet M and Stoquert J P 2003 *Nucl. Inst. Methods Phys. B* **209** 316
[3] Weller D and Moser A 1999 *IEEE Trans. Magn.* **35** 4423
[4] Weller D, Brandle H, Gorman G, Lin C J and Notarys H 1992 *Appl. Phys. Lett.* **61** 2726
[5] Ziegler F, Biersack J P, Littmark U 1985 *The Stopping and Range of Ions in Solids*, (New York : Pergamon) http://www.srim.org/
[6] Porter D A and Easterling K E 1992 *Phase Transformations in Metals and Alloys*, CRC Press
[7] Baldan A 2002 J. Mater. Sci. **37** 2171
[8] Mazzoldi P and Mattei G 2007 *Phys. Stat. Sol. A* **204** 621
[9] Cattaruzza E, Acapito F D, de Julian C F, De Lorenzi A, Gonella F, Mattei G, Maurizio C, Mazzoldi P, Padovani S, Scremin B F and Zontone F 2002 *Nucl. Inst. Methods Phys. B.***191** 406
[10] Mettei G, Maurizio C, de Julian C F, Mazzoldi P, Battaglin G, Canton P, Cattaruzza E, and Scian C 2006 *Nucl. Inst. Methods Phys. B* **250** 206
[11] Ocana M, Gonzalez-Elipe A R 1999 *Colloils surf. A: Physicochem. Eng. Aspects* **157** 315
[12] Ortega-Zarzosa G, Araujo-Andrade C, Compean-Jasso M E, Martinez J R and Ruiz F 2002 *J. Sol-Gel, Sci. Technol*. **24** 23